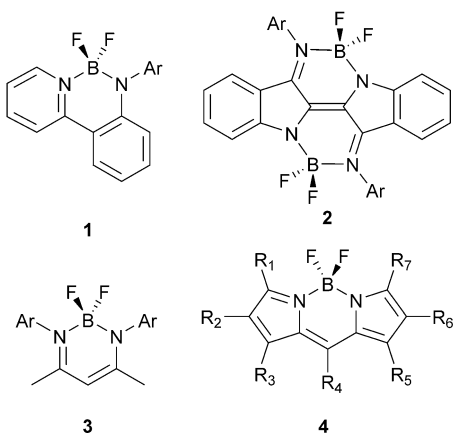


Boron Difluoride Dyes**Structurally Tunable 3-Cyanoformazanate Boron Difluoride Dyes**

Stephanie M. Barbon, Pauline A. Reinkeluers, Jacquelyn T. Price, Viktor N. Staroverov, and Joe B. Gilroy^{*[a]}

Abstract: The straightforward synthesis of a series of 3-cyanoformazanate boron difluoride dyes is reported. Phenyl, 4-methoxyphenyl and 4-cyanophenyl *N*-substituted derivatives were isolated and characterized by single-crystal X-ray crystallography, cyclic voltammetry, and UV/Vis spectroscopy. The compounds were demonstrated to possess tunable, substituent-dependent absorption, emission, and electrochemical properties, which were rationalized through electronic structure calculations.

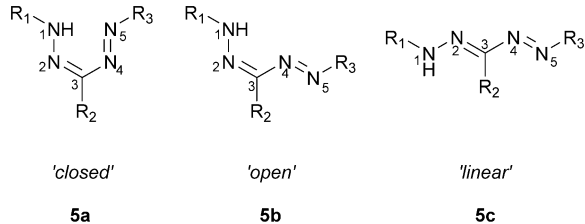
Boron complexes of chelating nitrogen-donor ligands have been widely studied as functional materials with structurally tunable properties.^[1,2] The most common of these complexes^[3] are produced via the coordination of boron difluoride $[BF_2]^+$ fragments with bidentate, monoanionic nitrogen-donor ligands such as anilido-pyridines,^[4] indigo-*N,N'*-diarylaminines,^[5] β -diketiminates,^[6] and dipyrins,^[7,8] resulting in structures **1–4**, respectively. These complexes are generally redox-active, highly absorbing and emissive, and chemically stable under diverse conditions.



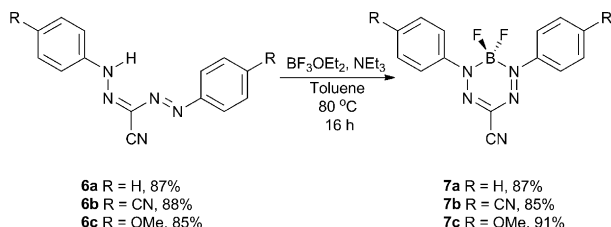
BF_2 complexes of dipyrin ligands (BODIPYs) **4** are by far the best known of these chelates due to their high fluorescence quantum yields, exceptional stability, and the ease of optical tuning through structural variation. BODIPYs have been used extensively as sensors, organic light-emitting diodes, and fluorescent imaging agents. For the latter application, fluorescent dyes should have high absorption coefficients, high fluorescence quantum yields, large Stokes shifts (SS), tunable emission and absorption spectra, and exceptional stability under a wide range of conditions.

Formazans, which can exist as 'closed', 'open', or 'linear' geometric isomers,^[9] **5a–c**, have long been used as dyes in the textile industry^[10] and as colorimetric indicators of cell activity.^[11] However, with the exception of a few recent examples, their coordination chemistry remains largely undeveloped.^[12,13]

Herein, we report the synthesis and characterization of BF_2 complexes of 3-cyanoformazanate ligands and demonstrate their readily tunable optical and electronic properties and potential utility as functional materials.



3-Cyanoformazans **6a–c**, which exist in the 'open' form due to the presence of a linear cyano substituent at the 3-position, were synthesized according to a published procedure (see Figure S1 and S2 in the Supporting Information).^[9] BF_2 complexes **7a–c** were produced by reacting 3-cyanoformazans with excess boron trifluoride diethyl etherate and triethylamine in refluxing toluene (Scheme 1, Figure S3–S8). It is noteworthy that the entire synthesis of **7a–c** involves only inexpensive and



Scheme 1. Synthesis of 3-cyanoformazanate BF_2 dyes **7a–c**.

[a] S. M. Barbon, P. A. Reinkeluers, Dr. J. T. Price, Prof. Dr. V. N. Staroverov, Prof. Dr. J. B. Gilroy
Department of Chemistry and the Centre for Advanced Materials and Biomaterials Research (CAMBR)
The University of Western Ontario
1151 Richmond St. N., London, Ontario, N6A 5B7 (Canada)
E-mail: joe.gilroy@uwo.ca

Supporting information for this article is available on the WWW under <http://dx.doi.org/10.1002/chem.201404297>.

commercially available reagents, consists of two straightforward high-yield steps, and requires only a few hours of hands-on bench time.

BF_2 dyes **7a–c** have diagnostic ^{11}B and ^{19}F NMR spectra, each exhibiting a 1:2:1 triplet in their ^{11}B NMR spectrum (**7a**: $\delta = -0.8$ ppm, **7b**: $\delta = -0.9$ ppm, and **7c**: $\delta = -0.7$ ppm) and a 1:1:1:1 quartet in their ^{19}F NMR spectrum (**7a**: $\delta = -133.6$ ppm, **7b**: $\delta = -129.6$ ppm, and **7c**: $\delta = -135.4$ ppm). The appearance of these signals was accompanied by the loss of the characteristic formazan NH signals in the ^1H NMR spectra. Dyes **7a–c** are air- and moisture-stable in the solid state and in solution. The solid-state structures of BF_2 complexes **7a–c** were determined by single-crystal X-ray diffraction (Figure 1, S9, S10, Table 1, S1). The solid-state structures show

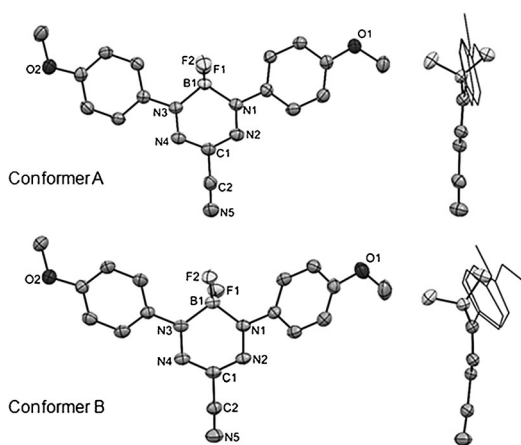


Figure 1. Solid-state structures of the two conformers of **7c**. Thermal ellipsoids are shown at 50% probability and hydrogen atoms are removed for clarity.

that the boron atoms in complexes **7a–c** are four-coordinate and adopt a slightly distorted tetrahedral geometry. Each complex has a delocalized formazanate backbone, with all C–N and N–N bonds approximately half way between the standard single and double bonds for the respective atoms involved.^[14]

The boron atoms are displaced slightly from the N_4 plane of the formazanate backbone, by 0.192 Å in **7a** and by 0.025 Å in **7b**. The unit cell of the crystalline structure of **7c** contains two molecular units in distinct conformations (Figure 1). Conformer A is almost flat and has a geometry very similar to **7a** and **7b**,

with the boron atom displaced from the N_4 plane by 0.143 Å. The second conformer, conformer B, is shaped like a dragonfly and has the boron atom displaced from the N_4 plane by 0.376 Å. The two conformers were found by electronic structure calculations to have very close energies (see below).

The aryl substituents of BF_2 complexes **7a**, **7b**, and **7c** (conformer A) are moderately twisted with respect to the formazanate backbone, with the angle between the N_4 plane and the plane defined by the *N*-aryl substituents ranging from 4.7 to 25.4°. For comparison, the same angles in conformer B of **7c** are 36.6–37.6°. Similar BF_2 complexes of other monoanionic, bidentate *N*-donor ligands exhibit significantly larger angles between the *N*-aryl substituents and the ligand backbones involved. For example, the aryl substituents in anilido-pyridine BF_2 complex **1** ($\text{Ar}=\text{phenyl}$) is twisted by 77°^[4b] while the aryl substituents in β -diketiminate BF_2 complexes are almost perpendicular to the ligand backbone, with twisting of 76–88°.^[6]

Table 2 summarizes the optical characterization data for BF_2 complexes **7a–c** collected in THF, CH_2Cl_2 , and toluene solutions. Each complex shows strong, substituent-dependent absorption of visible light due to $\pi \rightarrow \pi^*$ transitions with λ_{\max} values increasing from 502 nm (**7a**) to 515 nm (**7b**) to 572 nm (**7c**) in toluene (Figure 2, S11–S13). We note that the UV/Vis and emission spectra of **7b** ($\text{R}=\text{CN}$) are red-shifted relative to

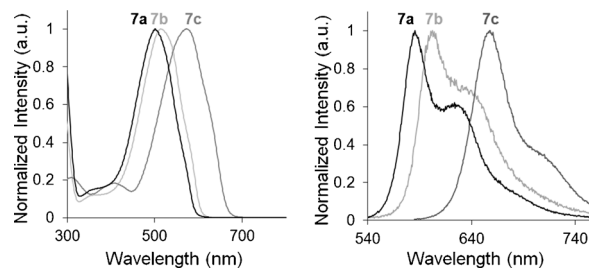


Figure 2. UV/Vis absorption (left) and emission (right) spectra of **7a–c** recorded in 10^{-5} M degassed toluene solutions.

7a ($\text{R}=\text{H}$), somewhat counterintuitively (see below). The 3-cyanoformazan ligands **6a–c** are non-emissive across a broad concentration range in THF, CH_2Cl_2 , and toluene. Under similar conditions, BF_2 complexes **7a–c** are highly emissive in the visible region, with λ_{em} of 586 nm ($\Phi=0.15$, SS=84 nm), 598 nm ($\Phi=0.14$, SS=83 nm), and 656 nm ($\Phi=0.77$, SS=84 nm) observed in toluene for **7a–c**, respectively. For comparison, a BF_2

Table 1. Selected bond lengths [Å] and angles [°] for BF_2 complexes **7a–c**, determined by X-ray diffraction.

7a ($\text{R}=\text{H}$) ^[a]	7b ($\text{R}=\text{CN}$)	7c ($\text{R}=\text{OMe}$)	
N1–N2, N3–N4	1.2900(15), 1.2948(15)	1.3017(15), 1.2945(15)	Conformer A
C1–N2, C1–N4	1.3408(17), 1.3379(17)	1.3289(17), 1.3382(17)	1.307(2), 1.304(2)
N1–B1, N3–B1	1.5748(18), 1.5771(17)	1.5714(18), 1.5817(18)	1.340(3), 1.335(3)
N1–N2–C1, N3–N4–C1	117.14(11), 117.30(11)	117.28(11), 117.76(11)	1.558(3), 1.567(3)
N2–C1–N4	129.33(12)	129.41(11)	1.563(3), 1.563(3)
N1–B1–N3	105.55(10)	105.65(10)	116.75(18), 116.90(18)
			116.21(17), 116.21(17)
			129.32(18)
			104.75(16)

[a] The second molecule in the unit cell of **7a** has a very similar geometry and is not reported here.

Table 2. Solution characterization data for BF_2 formazanate complexes **7a–c**.

	Solvent	λ_{max} [nm]	ϵ [$\text{M}^{-1}\text{cm}^{-1}$]	λ_{em} [nm]	Stokes shift [nm]	Stokes shift [cm^{-1}]	Quantum yield [Φ] ^[a]	E°_{red1} [V] ^[b]	E°_{red2} [V] ^[b]
7a ($\text{R}=\text{H}$)	THF	489	25 400	585	96	3356	0.05	−0.53	−1.68
	CH_2Cl_2	491	34 600	584	93	3243	0.09		
	toluene	502	30 400	586	84	2855	0.15		
7b ($\text{R}=\text{CN}$)	THF	497	22 600	590	93	3172	0.12	−0.21	−1.25
	CH_2Cl_2	499	22 400	589	90	3062	0.17		
	toluene	515	35 000	598	83	2695	0.14		
7c ($\text{R}=\text{OMe}$)	THF	556	33 400	662	106	2880	0.46	−0.68	−1.82
	CH_2Cl_2	558	35 300	661	103	2793	0.65		
	toluene	572	42 700	656	84	2239	0.77		

[a] Quantum yields were measured according to a previously published method^[18] using ruthenium tris(bipyridine) hexafluorophosphate as a relative standard,^[19] and corrected for detector non-linearity (Figure S15). [b] Cyclic voltammetry experiments were conducted in acetonitrile containing 1 mM analyte and 0.1 M tetrabutylammonium hexafluorophosphate at a scan rate of 100 mVs^{−1}. All voltammograms were referenced internally against the ferrocene/ferrocenium redox couple.

complex of a cyano-substituted pyridomethene ligand closely related to **7a** exhibits a smaller Stokes shift ($\Delta\lambda=6$ nm) and a quantum yield of 0.19.^[3b]

The effect of electron-withdrawing and electron-donating groups at the *N*-aryl substituents was investigated by cyclic voltammetry (Table 2). Each complex exhibited two reversible reduction waves (Figure 3) but only **7c** gave rise to an irrever-

To rationalize the trends in the UV/Vis spectra and cyclic voltammograms of **7a–c**, we calculated the molecular orbitals and the lowest electronic excitation energies of these compounds with density functional theory (DFT) methods. All calculations were carried out with the Gaussian 09 program^[15] using the M06 functional^[16] and the 6-311+G* basis set, in vacuum and in the presence of toluene as a solvent. The solvent was simulated implicitly using the self-consistent reaction field (SCRF) method with the polarizable continuum model. The M06 functional was chosen because it has the best performance in time-dependent DFT calculations of valence excited states among 24 common density-functional approximations.^[17]

Because the molecules of **7a–c** appear to be relatively planar in the crystalline phase, we first optimized their geometries under the constraint of C_{2v} symmetry, but none of the C_{2v} structures turned out to be a minimum on the potential energy surface. Unconstrained geometry optimization yielded structures of C_s symmetry (shaped like dragonflies) which were confirmed by vibrational analysis to be true minima. The C_s structures are more stable than the corresponding C_{2v} structures by only 3–5 kJ mol^{−1}, meaning that the planar conformations are readily accessible (see Table S2). The gas-phase and SCRF calculations for C_{2v} and C_s structures led to the same conclusions, so we will discuss here only the implicitly solvated structures, while the gas-phase results are relegated to the Supporting Information (Table S3).

To understand why the electron-withdrawing CN group red-shifts (not blue-shifts) the UV absorption band for **7b** ($\text{R}=\text{CN}$) relative to **7a** ($\text{R}=\text{H}$), we note that the HOMO and LUMO of compounds **7a–c** are π -conjugated (see Figure 4, S16–S18). Re-

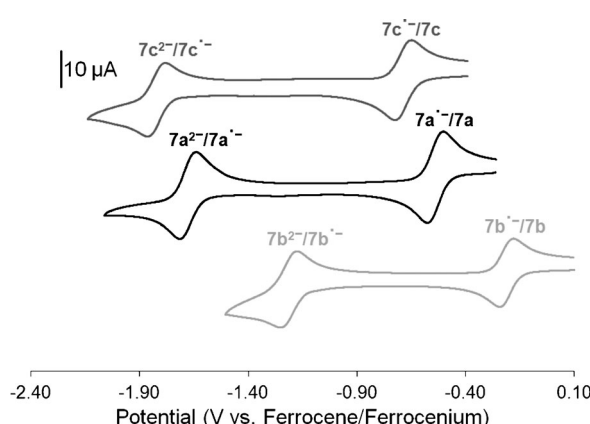


Figure 3. Cyclic voltammograms of **7a–c** recorded at 100 mVs^{−1} in a 1 mM acetonitrile solution containing 0.1 M tetrabutylammonium hexafluorophosphate.

sible oxidation event within the electrochemical window of acetonitrile (see Figure S14). The reduction potentials followed the expected trend based on the *para*-substituent introduced at the aryl rings. BF_2 complex **7a** ($\text{R}=\text{H}$) is reduced to a radical anion and then a dianion at −0.53 V and −1.68 V against the ferrocene/ferrocenium redox couple, while **7b** ($\text{R}=\text{CN}$) was reduced at −0.21 V and −1.25 V and **7c** ($\text{R}=\text{OMe}$) was reduced at −0.68 V and −1.82 V. Previous reports of the electrochemistry of main-group and transition-metal complexes of formazanate ligands have demonstrated reversible reduction to the radical anion^[12a,c,d] and dianion^[13] forms. In this case, BF_2 complexes **7a–c** also exhibit a second reversible one-electron reduction to the dianion.

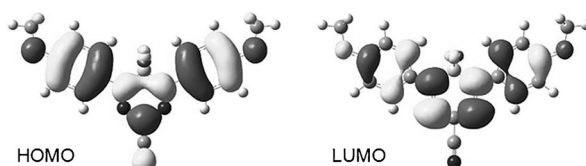


Figure 4. HOMO and LUMO for **7c** (C_{2v}).

placement of an H atom (**7a**) with a $\text{C}\equiv\text{N}$ group (**7b**) increases the spatial extent of π -conjugation in the molecule and therefore lowers the energy of the $\pi\rightarrow\pi^*$ transition. The same effect is observed for monosubstituted benzenes, $\text{Ph}-\text{R}$, where the energy of the $\pi\rightarrow\pi^*$ transition as a function of substituent also decreases in the order $\text{R}=\text{H} > \text{R}=\text{CN} > \text{R}=\text{OMe}$ (Figure S19).

In contrast to the UV/Vis absorption spectra, the cyclic voltammograms of **7a–c** should correlate not with electronic excitation energies but with the electron-acceptor capacity of the substituents, which is characterized by the LUMO energies. Experimentally, the peak-current potentials decrease in the order **7b** ($\text{R}=\text{CN}$) $>$ **7a** ($\text{R}=\text{H}$) $>$ **7c** ($\text{R}=\text{OMe}$) (Table 2). This trend is fully consistent with the calculated LUMO energies of the substituted complexes (Table 3). Thus, electronic structure calculations support all experimental observations.

Table 3. Lowest electronic excitations and HOMO/LUMO energies of the substituted BF_2 complexes in toluene solution calculated at the M06/6-311+G* level of theory using the SCRF method.

		Lowest excitation energy ^[a] [eV]	ϵ_{HOMO} [nm]	ϵ_{LUMO} [eV]	HOMO-LUMO gap [eV]
C_{2v} structures	7a ($\text{R}=\text{H}$)	2.39	518	-6.94	3.05
	7b ($\text{R}=\text{CN}$)	2.36	526	-7.49	3.01
	7c ($\text{R}=\text{OMe}$)	2.12	584	-6.34	2.71
C_s structures	7a ($\text{R}=\text{H}$)	2.65	468	-7.12	3.36
	7b ($\text{R}=\text{CN}$)	2.57	483	-7.62	3.26
	7c ($\text{R}=\text{OMe}$)	2.30	538	-6.47	2.93

[a] Computed using time-dependent DFT. The first excited states of the C_{2v} and C_s structures have B_2 and A'' symmetry, respectively.

In conclusion, we have described the straightforward synthesis of a series of 3-cyanoformazanate BF_2 dyes exhibiting variable redox, absorption, and emission properties, which can be tuned through simple changes of *N*-aryl substituents. Based on these factors, we envision this new class of dyes to be of significant interest in the optical imaging and functional materials fields. Efforts to synthesize water-soluble analogs of 3-cyanoformazanate dyes and to explore the potential utility of 3-cyanoformazanate BF_2 dyes in materials-based applications are currently underway.

Acknowledgements

This work was supported by the Natural Sciences and Engineering Research Council of Canada (NSERC) Discovery Grants (J. B. G. and V. N. S.), Canada Graduate Scholarships program (S. M. B.), and by The University of Western Ontario. We thank Prof. Elizabeth R. Gillies for access to instruments in her lab and Prof. Mark Workentin for helpful discussions.

Keywords: boron • density functional calculations • electrochemistry • emission spectroscopy • X-ray diffraction

- [1] D. Frath, J. Massue, G. Ulrich, R. Ziessel, *Angew. Chem.* **2014**, *126*, 2322–2342; *Angew. Chem. Int. Ed.* **2014**, *53*, 2290–2310.
- [2] For example: a) F. Cheng, F. Jäkle, *Chem. Commun.* **2010**, *46*, 3717–3719; b) G. M. Fischer, E. Daltrozzo, A. Zumbusch, *Angew. Chem.* **2011**, *123*, 1442–1445; *Angew. Chem. Int. Ed.* **2011**, *50*, 1406–1409; c) E. Firinci, J. I. Bates, I. M. Riddlestone, N. Phillips, S. Aldridge, *Chem. Commun.* **2013**, *49*, 1509–1511; d) J.-S. Lu, S.-B. Ko, N. R. Walters, Y. Kang, F. Sauviroi, S. Wang, *Angew. Chem.* **2013**, *125*, 4642–4646; *Angew. Chem. Int. Ed.* **2013**, *52*, 4544–4548; e) D. Frath, A. Poirel, G. Ulrich, A. De Nicola, R. Ziessel, *Chem. Commun.* **2013**, *49*, 4908–4910.
- [3] For example: a) T. W. Hudnall, F. P. Gabbaï, *Chem. Commun.* **2008**, 4596–4597; b) Y. Kubota, T. Tsuzuki, K. Funabiki, M. Ebihara, M. Matsui, *Org. Lett.* **2010**, *12*, 4010–4013; c) S. Hapuarachchige, G. Montaño, C. Ramesh, D. Rodriguez, L. H. Henson, C. C. Williams, S. Kadavakkollu, D. L. Johnson, C. B. Shuster, J. B. Arterburn, *J. Am. Chem. Soc.* **2011**, *133*, 6780–6790; d) Y. Yang, R. P. Hughes, I. Aprahamian, *J. Am. Chem. Soc.* **2012**, *134*, 15221–15224; e) Y. Yang, X. Su, C. N. Carroll, I. Aprahamian, *Chem. Sci.* **2012**, *3*, 610–613; f) W. Li, W. Lin, J. Wang, X. Guan, *Org. Lett.* **2013**, *15*, 1768–1771; g) I.-S. Tamgho, A. Hasheminasab, J. T. Engle, V. N. Nemykin, C. J. Ziegler, *J. Am. Chem. Soc.* **2014**, *136*, 5623–5626.
- [4] a) Y. Ren, X. Liu, W. Gao, H. Xia, L. Ye, Y. Mu, *Eur. J. Inorg. Chem.* **2007**, 1808–1814; b) J. F. Araneda, W. E. Piers, B. Heyne, M. Parvez, R. McDonald, *Angew. Chem.* **2011**, *123*, 12422–12425; *Angew. Chem. Int. Ed.* **2011**, *50*, 12214–12217.
- [5] a) G. Nawn, K. M. Waldie, S. R. Oakley, B. D. Peters, D. Mandel, B. O. Patrick, R. McDonald, R. G. Hicks, *Inorg. Chem.* **2011**, *50*, 9826–9837; b) G. Nawn, S. R. Oakley, M. B. Majewski, R. McDonald, B. O. Patrick, R. G. Hicks, *Chem. Sci.* **2013**, *4*, 612–621.
- [6] a) F. P. Macedo, C. Gwengo, S. V. Lindeman, M. D. Smith, J. R. Gardiner, *Eur. J. Inorg. Chem.* **2008**, 3200–3211; b) S. M. Barbon, V. N. Staroverov, P. D. Boyle, J. B. Gilroy, *Dalton Trans.* **2014**, *43*, 240–250.
- [7] For recent reviews: a) A. Loudet, K. Burgess, *Chem. Rev.* **2007**, *107*, 4891–4932; b) G. Ulrich, R. Ziessel, A. Harriman, *Angew. Chem.* **2008**, *120*, 1202–1219; *Angew. Chem. Int. Ed.* **2008**, *47*, 1184–1201; c) N. Boens, V. Leen, W. Dehaen, *Chem. Soc. Rev.* **2012**, *41*, 1130–1172.
- [8] For example: a) T. Lazarides, T. M. McCormick, K. C. Wilson, S. Lee, D. W. McCamant, R. Eisenberg, *J. Am. Chem. Soc.* **2010**, *132*, 350–364; b) O. Altan Bozdemir, S. Erbas-Cakmak, O. O. Ekiz, A. Dana, E. U. Akkaya, *Angew. Chem.* **2011**, *123*, 11099–11104; *Angew. Chem. Int. Ed.* **2011**, *50*, 10907–10912; c) J. C. T. Carlson, L. G. Meimetsis, S. A. Hilderbrand, R. Weissleder, *Angew. Chem.* **2013**, *125*, 7055–7058; *Angew. Chem. Int. Ed.* **2013**, *52*, 6917–6920; d) C. Zhang, J. Zhao, S. Wu, Z. Wang, W. Wu, J. Ma, S. Guo, L. Huang, *J. Am. Chem. Soc.* **2013**, *135*, 10566–10578.
- [9] J. B. Gilroy, P. O. Otieno, M. J. Ferguson, R. McDonald, R. G. Hicks, *Inorg. Chem.* **2008**, *47*, 1279–1286.
- [10] For example: a) Y. Gök, *Dyes Pigm.* **1989**, *11*, 101–107; b) M. Szymczyk, A. El-Shafei, H. S. Freeman, *Dyes Pigm.* **2007**, *72*, 8–15.
- [11] For example: a) C. J. Goodwin, S. J. Holt, S. Downes, N. J. Marshall, *J. Immunol. Methods* **1995**, *179*, 95–103; b) W. M. Frederiks, J. van Marle, C. van Oven, B. Comin-Anduix, M. Cascante, *J. Histochem. Cytochem.* **2006**, *54*, 47–52.
- [12] For example: a) J. B. Gilroy, M. J. Ferguson, R. McDonald, B. O. Patrick, R. G. Hicks, *Chem. Commun.* **2007**, 126–128; b) J. B. Gilroy, B. O. Patrick, R. McDonald, R. G. Hicks, *Inorg. Chem.* **2008**, *47*, 1287–1294; c) S. Hong, L. M. R. Hill, A. K. Gupta, B. D. Naab, J. B. Gilroy, R. G. Hicks, C. J. Cramer, W. B. Tolman, *Inorg. Chem.* **2009**, *48*, 4514–4523; d) M.-C. Chang, T. Dann, D. P. Day, M. Lutz, G. G. Wildgoose, E. Otten, *Angew. Chem.* **2014**, *126*, 4202–4206; *Angew. Chem. Int. Ed.* **2014**, *53*, 4118–4122.
- [13] For a transmetallation route to triaryl formazante BF_2 complexes, see: M.-C. Chang, E. Otten, *Chem. Commun.* **2014**, *50*, 7431.
- [14] CRC Handbook of Chemistry and Physics, CRC Press, Boca Raton, **2012**.
- [15] Gaussian 09, Revision B.01, M. J. Frisch, G. W. Trucks, H. B. Schlegel, G. E. Scuseria, M. A. Robb, J. R. Cheeseman, G. Scalmani, V. Barone, B. Mennucci, G. A. Petersson, H. Nakatsuji, M. Caricato, X. Li, H. P. Hratchian, A. F. Izmaylov, J. Bloino, G. Zheng, J. L. Sonnenberg, M. Hada, M. Ehara,

- K. Toyota, R. Fukuda, J. Hasegawa, M. Ishida, T. Nakajima, Y. Honda, O. Kitao, H. Nakai, T. Vreven, J. A. Montgomery, Jr., J. E. Peralta, F. Ogliaro, M. Bearpark, J. J. Heyd, E. Brothers, K. N. Kudin, V. N. Staroverov, R. Kobayashi, J. Normand, K. Raghavachari, A. Rendell, J. C. Burant, S. S. Iyengar, J. Tomasi, M. Cossi, N. Rega, J. M. Millam, M. Klene, J. E. Knox, J. B. Cross, V. Bakken, C. Adamo, J. Jaramillo, R. Gomperts, R. E. Stratmann, O. Yazyev, A. J. Austin, R. Cammi, C. Pomelli, J. W. Ochterski, R. L. Martin, K. Morokuma, V. G. Zakrzewski, G. A. Voth, P. Salvador, J. J. Dannenberg, S. Dapprich, A. D. Daniels, Ö. Farkas, J. B. Foresman, J. V. Ortiz, J. Cioslowski, D. J. Fox. Gaussian, Inc., Wallingford CT, 2009.
- [16] Y. Zhao, D. G. Truhlar, *Theor. Chem. Acc.* **2008**, *120*, 215–241.
[17] S. S. Leang, F. Zahariev, M. S. Gordon, *J. Chem. Phys.* **2012**, *136*, 104101.
[18] S. Fery-Forgues, D. Lavabre, *J. Chem. Educ.* **1999**, *76*, 1260–1264.
[19] K. Suzuki, A. Kobayashi, S. Kaneko, K. Takehira, T. Yoshihara, H. Ishida, Y. Shiina, S. Oishi, S. Tobita, *Phys. Chem. Chem. Phys.* **2009**, *11*, 9850–9860.

Received: July 8, 2014

Published online on July 25, 2014